

# Registration of Under-Sampled Images via Higher Resolution Spectrum Restoration

Qiang Song<sup>†</sup>, Ruiqin Xiong<sup>†</sup>, Xinfeng Zhang<sup>‡</sup>, Siwei Ma<sup>†</sup>, Wen Gao<sup>†</sup>

<sup>†</sup>Institute of Digital Media, Peking University, Beijing 100871, China

<sup>‡</sup>Rapid-Rich Object Search Lab, Nanyang Technological University, Singapore

Email: {songqiang, rqxiong, swma, wgao}@pku.edu.cn, zhangxf@ntu.edu.sg

**Abstract**—High accuracy image registration is critical for the success of multi-frame super-resolution. Conventionally, the shift between images are estimated directly based on the under-sampled low-resolution (LR) image data. However, the high-frequency of LR data is unreliable due to the aliasing effect of sub-sampling, which will deteriorate the accuracy of registration. This paper proposes to resolve the aliasing by converting the LR images to high-resolution (HR) domain and then perform registration on the restored HR spectrum. To recover the HR spectrum for each corresponding LR image, we fuse the LR images into one HR image and project the estimation difference back to the reconstructed HR spectrum iteratively. To address the unequal reliabilities of different restored frequencies, weighted least square is employed to improve the precision of registration. Experimental results show that the proposed method can outperform other existing methods and improve the quality of super-resolution image.

**Index Terms**—Image registration, super-resolution, aliased image, spectrum restoration, weighted least square

## I. INTRODUCTION

Image super-resolution has been studied widely over the past two decades. Based on the sampling theorem, the original high-resolution (HR) image can not be generally reconstructed using only a single under-sampled low-resolution (LR) image. However, several LR images sampled from the same scene with relative shifts allow the possibility of reconstructing the HR image. Tsai and Huang [1] first proposed a system that describes the relationship between LR images and a HR image using relative shifts between LR images. Most super-resolution (SR) methods are performed in two stages: registration and reconstruction. Generally, the performance of SR algorithms relies heavily on the accuracy of estimated shifts. However, high precision registration is difficult to achieve due to the presence of alias caused by under-sampling.

Various image registration methods have been proposed in literature [2]–[13]. Based on the Fourier shift theorem, Vandewalle [2] uses only the low frequency spectrum instead of the whole spectrum to reduce the influence of alias. Murat Balci

This work was supported by the National Basic Research Program of China (973 Program, 2015CB351800), National Natural Science Foundation of China (61370114, 61421062), Beijing Natural Science Foundation (4132039), Research Fund for the Doctoral Program of Higher Education (20120001110090) and also by the Cooperative Medianet Innovation Center.

[3] and Jinchang Ren [4] apply a phase correlation technique to find the shifts between images. Keren [5] proposes a method based on Taylor expansions. Although these methods work well for alias-free images, the registration accuracy is far below the demand for aliased images.

In this paper, we propose a high-precision frequency-domain registration method for aliased images. Due to the presence of alias, high-frequency components of LR images are unreliable. Meanwhile, we show in the paper that components of higher frequency offer better resolving capability for estimating the shift. As a result, registering the LR images directly cannot achieve high estimation precision. Unlike conventional methods, the proposed method tries to restore the high-resolution spectrum from the whole set of LR images and register them in the higher resolution with less alias. The HR spectrum is iteratively restored based on a back projection scheme. Furthermore, we employ weighted least square to handle the unequal reliability of different frequency coefficients.

This paper is organized as follows. Section II gives some analysis of the aliased image registration problem. Section III presents the framework of our method. Section IV explains some details of the proposed scheme. Experimental results are then given in Section V and Section VI concludes the paper with a few remarks.

## II. PRELIMINARY ANALYSIS

Assume we have two images  $f_1$  and  $f_2$  captured from the same scene with horizontal and vertical shifts,  $d_1$  and  $d_2$ . The relationship between them can be described in the frequency domain as follows:

$$F_1(\mathbf{u}) = e^{j2\pi\mathbf{u}^T\mathbf{d}}F_2(\mathbf{u}). \quad (1)$$

where  $\mathbf{u} = (u_1, u_2)^T$  is frequency point and  $\mathbf{d} = (d_1, d_2)^T$  is the shift vector. This translates to the following phase equations:

$$2\pi\mathbf{u}^T\mathbf{d} = \angle(F_2(\mathbf{u})/F_1(\mathbf{u})) \pmod{2\pi} \quad (2)$$

Eq. (2) actually represents a plane with slope  $\mathbf{d}$  and we call it phase difference plane (See Fig.1(a)). The parameter  $\mathbf{d}$  can thus be computed as the slope of the phase difference  $\angle(F_2(\mathbf{u})/F_1(\mathbf{u}))$ . More generally, we usually use a least-square estimator to make the estimation less sensitive to noise:

$$\Delta\mathbf{x} = \arg \min_{\Delta\mathbf{x}} \|2\pi\mathbf{U}\mathbf{d} - \Psi\|_2^2 \quad (3)$$

$\mathbf{U}$  and  $\Psi$  are as follows where the index  $i$  denotes the  $i^{th}$  frequency point:

$$\mathbf{U} = \begin{bmatrix} \mathbf{u}_1^T \\ \vdots \\ \mathbf{u}_i^T \\ \vdots \\ \mathbf{u}_N^T \end{bmatrix}, \quad \Psi = \begin{bmatrix} \angle(F_2(\mathbf{u}_1)/F_1(\mathbf{u}_1)) \\ \vdots \\ \angle(F_2(\mathbf{u}_i)/F_1(\mathbf{u}_i)) \\ \vdots \\ \angle(F_2(\mathbf{u}_N)/F_1(\mathbf{u}_N)) \end{bmatrix} \quad (4)$$

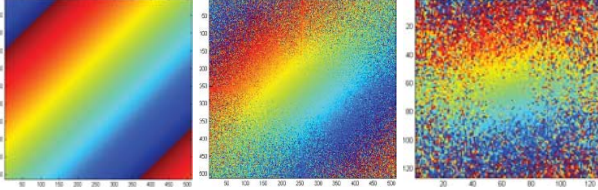


Fig. 1. Phase difference plane. From left to right: (a) clean; (b) noisy; (c) aliased

Actually, Eq. (2) is valid only for the ideal case. In practice, we usually have to take the following issues into account: (1) the images may be sampled under the Nyquist rate, and (2) the images may contain noise. In such cases, the phase difference plane will be disturbed, as illustrated in Fig.1(b) and (c). This brings challenges for registration.

#### A. Role of High-Frequency in Image Registration

To simplify the description, we focus our discussion on one-dimensional (1-D) signal, but all the conclusions can be applied to the 2-D case.

For 1-D signal, formula (2) changes to a scalar form:

$$2\pi \cdot u \cdot d = \Theta_u \quad (5)$$

where  $\Theta_u = \angle(F_2(u)/F_1(u))$ . Typically, the signals are influenced by noise or aliasing effect and errors will exist in  $\Theta_u$ :

$$2\pi \cdot u \cdot d = \Theta_u + \Delta\Theta_u \quad (6)$$

Consequently, the error in shift estimation can be expressed as follows:

$$\Delta d = \left| \tilde{d} - d \right| = \frac{\left| \tilde{\Theta}_u - \Theta_u \right|}{2\pi \cdot u} = \frac{|\Delta\Theta_u|}{2\pi \cdot u} \quad (7)$$

We can see from the above formulation that larger  $u$  corresponds to smaller  $\Delta d$  for a given  $\Delta\Theta_u$ . In other words, the coefficients of higher frequency have better resolving capability in registration. Low-frequency components are less useful than the high-frequency components, when they are equally reliable. This indicates the benefit to use reliable high-frequency coefficients.

#### B. Super-Resolution from Aliased Images

Assume we have a periodic, band-limited continuous image  $f(\mathbf{x})$  with period of 1 and its Fourier decomposition can be expressed as follows

$$f(\mathbf{x}) = \sum_{k_1=-K_1}^{K_1} \sum_{k_2=-K_2}^{K_2} \alpha_{\mathbf{k}} e^{j2\pi\mathbf{k}^T\mathbf{x}}, \quad (8)$$

where  $\alpha_{\mathbf{k}}$  are the  $L_1L_2 = (2K_1 + 1)(2K_2 + 1)$  Fourier coefficients of  $f(\mathbf{x})$  and  $\mathbf{k} = (k_1, k_2)^T$ ,  $\mathbf{x} = (x_1, x_2)^T$ .

Through moving the sampling camera, the continuous image is sampled with  $M$  shifted images at horizontal and vertical frequencies  $N_1$  and  $N_2$ . The horizontal and vertical shifts are  $\mathbf{t}_m = (t_{m,1}, t_{m,2})$ ,  $1 < m < M$ . The sampled image can be expressed using  $f(\mathbf{x})$  as

$$y_m(\mathbf{n}) = f\left(\frac{n_1}{N_1} + t_{m,1}, \frac{n_2}{N_2} + t_{m,2}\right) \quad (9)$$

$$= \sum_{k_1=-K_1}^{K_1} \sum_{k_2=-K_2}^{K_2} \alpha_{\mathbf{k}} e^{j2\pi(k_1 t_{m,1} + k_2 t_{m,2})} e^{j2\pi(k_1 \frac{n_1}{N_1} + k_2 \frac{n_2}{N_2})} \quad (10)$$

The above formula describes the observation model, i.e., the HR image is firstly shifted and then these shifted HR images are sampled to generate the LR images. In the following, these shifted HR images are defined as  $f_m$ . By using lexicographic ordering for the indices, a matrix vector form of the observation model is as follows

$$\mathbf{y}_m = \Phi_{\mathbf{t}_m} \alpha, \quad (11)$$

where  $\Phi_{\mathbf{t}_m}$  is an  $L_1L_2 \times N_1N_2$  sampled basis matrix and  $\mathbf{y}_m$ ,  $\alpha$  are  $N_1N_2 \times 1$  and  $L_1L_2 \times 1$  vectors rearranged by lexicographic ordering. If all the sets of  $\mathbf{y}_m$  are combined into a single vector  $\mathbf{y}$  and, similarly, the basis matrices are combined into  $\Phi_{\mathbf{t}}$ , with  $\mathbf{t} = \{\mathbf{t}_1, \mathbf{t}_2, \dots, \mathbf{t}_M\}$  denoting the offset vector, this can be written as follows:

$$\mathbf{y} = \begin{bmatrix} \mathbf{y}_1 \\ \mathbf{y}_2 \\ \vdots \\ \mathbf{y}_M \end{bmatrix} = \begin{bmatrix} \Phi_{\mathbf{t}_1} \\ \Phi_{\mathbf{t}_2} \\ \vdots \\ \Phi_{\mathbf{t}_M} \end{bmatrix} \alpha = \Phi_{\mathbf{t}} \alpha. \quad (12)$$

Therefore, the reconstruction of a HR image requires us to determine  $\Phi_{\mathbf{t}}$  and solve this inverse problem. It is well known that the HR image can be perfectly reconstructed if the shifts between the LR images are known or well estimated.

### III. THE PROPOSED FRAMEWORK

Instead of directly using LR images, we use the shifted HR images  $\{f_m\}$  defined in section II-B to estimate the shifts between the LR images. The proposed scheme is shown in Fig. 2. Given a sequence of aliased images  $\{y_m\}$ , we firstly use an existing method to get an initial estimation of shifts  $\{\mathbf{t}_m^0\}$ . Then an HR image  $f_0$  is reconstructed based on the methodology described in section II-B. Afterwards, the shifted HR images  $\{f_m\}$  are generated using the relationship between alias-free shifted images (See formula (1)). These two steps coarsely recover the aliased spectrum of the LR images. However, the obtained spectrum is not always reliable because of the unavoidable errors in  $\{\mathbf{t}_m^0\}$ . Therefore, we use a back-projection scheme to modify the spectrums of  $\{f_m\}$  here. After the modification,  $\{f_m\}$  is registered using a registration method for the noisy but alias-free images. The above process can be iterative. So we repeat the process until the registration errors is small enough.

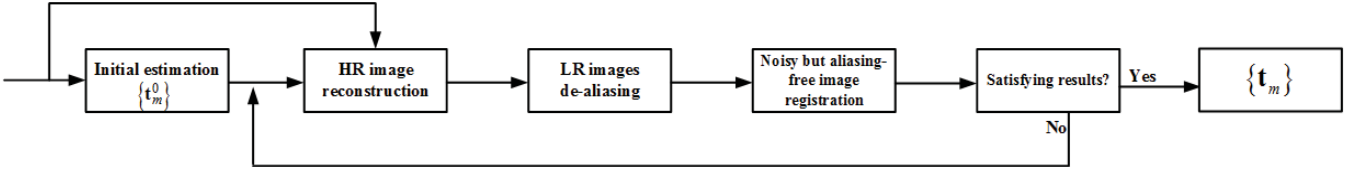


Fig. 2. The proposed framework.

In our scheme, the main technical contributions in this paper are the de-aliasing module and image registration module. We will discuss how to de-alias the LR image set and do registration in the next section.

#### IV. DETAILS OF THE FRAMEWORK

##### A. Spectrum Restoration via Back-Projection

Because of alias, the spectrums of under-sampled low-resolution (LR) images are overlapped and unreliable. Under this circumstance, the use of high-frequency coefficients will destroy the estimation. How can we reuse these helpful data? One feasible scheme is de-aliasing and recovering the high-frequency spectrum of the LR images. The interior of the de-

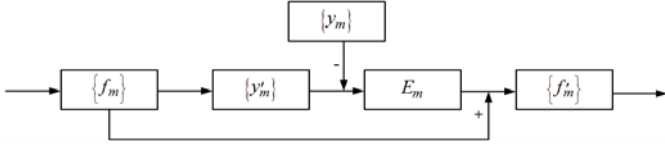


Fig. 3. Illustration of the spectrum restoration procedure.

aliasing module is shown in Fig.3. After the shifted HR images  $\{f_m\}$  have been generated, they are down-sampled to generate the 'false' LR images  $\{y'_m\}$ .

Then errors between the original LR images  $\{y_m\}$  and 'false' LR images  $\{y'_m\}$  can be computed:

$$E_m = y_m - y'_m \quad (13)$$

Where  $E_m$  is the error between  $y_m$  and  $y'_m$ .

As we all know, the low-frequency parts take up most of the energy of one image. So  $E_m$  is mainly caused by the wrongly estimated low-frequency parts. To make  $\{f_m\}$  more reliable, the errors are back-projected to  $\{f_m\}$  in the Fourier domain:

$$\mathcal{F}(f'_m) = \mathcal{F}(f_m) + P(\mathcal{F}(E_m)) \quad (14)$$

The operation  $P(\cdot)$  means padding  $E_m$  with zeros to the same size of  $f_m$  while the zero-frequency of  $f_m$  and  $E_m$  are both in the center. This process is illustrated in Fig.4. Now the more

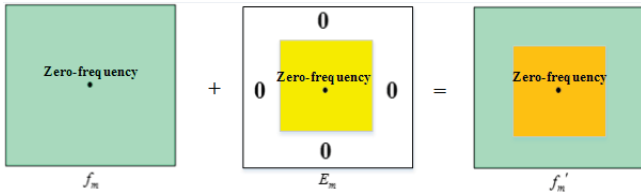


Fig. 4. Example of error back-projection (scale=2)

reliable  $\{f_m\}$  are obtained and the aliased image registration problem is equivalent to estimate the shifts between these HR images.

##### B. Reliability Based Image Registration

As soon as the LR images are coarsely de-aliased, the high-frequency coefficients can participate in registration. However, this is not sufficient to attain high precision in registration. Though more reliable  $\{f_m\}$  have been obtained, the high-frequency coefficients can not be reliable completely. In this case, the reliability of the frequency coefficients should be considered.

As shown in Fig.1 (b) and (c), we find out that some of the frequency components (especially the low-frequency parts) are cleaner than others. It is because the amplitudes of these components are generally much larger and can not be easily changed by noise or aliasing artifacts. This illustrates that those slightly disturbed frequency components should contribute more while those severely disturbed ones contribute less. If we regard aliasing artifacts as a special case of noise interference, the algorithm should mask out contributions from spectral components whose amplitudes are small compared to the noise amplitude, regardless of whether they occur at low or high frequencies. Then the objective function (3) should change to the following weighted least squares form:

$$\Delta \mathbf{x} = \arg \min_{\Delta \mathbf{x}} \|\mathbf{W}^{\frac{1}{2}} \cdot \Upsilon_{\xi}(2\pi \cdot \mathbf{U} \cdot \mathbf{d} - \Psi)\|_2^2 \quad (15)$$

$\mathbf{W}$  is a diagonal matrix with  $\mathbf{W}(i, i) = w_i$ .  $w_i$  is the weight of the  $i^{th}$  frequency coefficient.  $\Upsilon_{\xi}$  is an operator with threshold  $\xi$  which masks out the contributions from unreliable coefficients. As demonstrated in [7], under the assumption of Gaussian noise,  $w_i$  can be computed as follows:

$$w_i = \frac{1}{2\sigma^2} \approx \frac{|\hat{F}(\mathbf{u}_i)|^2}{2\sigma_n^2} \quad (16)$$

where  $\hat{F}(\mathbf{u}_i) = \text{mean}(|F_1(\mathbf{u}_i)|, |F_2(\mathbf{u}_i)|)$  and  $\sigma_n$  is the standard variance of  $E_m$ . Here we use the same suggestion to compute the weights.

#### V. EXPERIMENTAL RESULTS

In this section, simulated experiments are performed on real images to evaluate the performance of the proposed method. To make the image circularly symmetric and avoid boundary effects, the test images are multiplied by a Tukey window. Five shifted and aliased low-resolution images are created from an original high resolution image with a scale of 2 in both dimensions. The shift parameters are generated randomly from

TABLE I  
COMPARISON OF THE AVERAGE ABSOLUTE ERROR

Images	method[2]	Keren[5]	method [6])	Proposed
Castle	0.0884	0.0311	1.7375	<b>0.0093</b>
Airplane	0.1021	0.0186	1.8898	<b>0.0043</b>
Motor	0.2737	0.0303	1.7386	<b>0.0096</b>
Parrot	0.1506	0.0199	1.6189	<b>0.0057</b>
Pepper	0.1770	0.0352	1.7321	<b>0.0106</b>
Lenna	0.1936	0.0280	1.7321	<b>0.0080</b>

the interval  $[0, 2]$ . The threshold is empirically chosen as 0.1 for the registration module. For other comparative methods, we choose the empirical parameter settings, which give the best performance for the images. The proposed method is compared with three representative aliased image registration methods. As shown in Table 1, the four registration results are reported in each cell. In the experiments, 100 simulations were repeated and then the results are averaged for each method to make the experiments more stable and convincing. The average absolute errors (pixel) are computed as a criterion to measure the performance of registration. In the following, the shifts were estimated using our method and the high resolution image was reconstructed from the low resolution images. Due to the limited space, the results of four images are shown in Fig.5. As can be seen in Table 1, our proposed method outperforms all the four methods evidently. Fig.5 shows that the original double resolution image is perfectly reconstructed using our registration method. All the results prove that our method can satisfy the demand for super-resolution.

## VI. CONCLUSIONS

This paper presents a new scheme for registration of aliased image. The proposed technique discusses the role of high-frequency components in registration. Based on the analysis, we use the high resolution versions of the LR images instead to estimate the relative shifts between the LR images. These high resolution images are estimated and a weighted least squares method is proposed to improve the accuracy. Experiments show that the proposed approach can achieve high-precision in face of alias.

## REFERENCES

- [1] R. Tsai and T. S. Huang, "Multiframe image restoration and registration," *Advances in Computer Vision and Image Processing*, vol. 1, no. 2, pp. 317–339, 1984.
- [2] P. Vandewalle, S. Süsstrunk, and M. Vetterli, "A frequency domain approach to registration of aliased images with application to super-resolution," *EURASIP Journal on Applied Signal Processing*, vol. 2006, pp. 233–233, 2006.
- [3] M. Balci and H. Foroosh, "Subpixel estimation of shifts directly in the fourier domain," *IEEE Transactions on Image Processing*, vol. 15, no. 7, pp. 1965–1972, 2006.
- [4] J. Ren, J. Jiang, and T. Vlachos, "High-accuracy sub-pixel motion estimation from noisy images in fourier domain," *IEEE Transactions on Image Processing*, vol. 19, no. 5, pp. 1379–1384, 2010.
- [5] D. Keren, S. Peleg, and R. Brada, "Image sequence enhancement using sub-pixel displacements," in *Proceedings of Computer Vision and Pattern Recognition (CVPR)*, 1988, pp. 742–746.



Fig. 5. Reconstruction results. Left: one of the 5 LR images. Right: reconstructed image.

- [6] P. Vandewalle, L. Sbaiz, J. Vandewalle, and M. Vetterli, "Super-resolution from unregistered and totally aliased signals using subspace methods," *IEEE Transactions on Signal Processing*, vol. 55, no. 7, pp. 3687–3703, 2007.
- [7] Q. Song, R. Xiong, S. Ma, X. Fan, and W. Gao, "High accuracy sub-pixel image registration under noisy condition," in *IEEE International Symposium on Circuits and Systems (ISCAS)*, 2015, pp. 1674–1677.
- [8] X. Zhang, R. Xiong, S. Ma, G. Li, and W. Gao, "Video super-resolution with registration-reliability regulation and adaptive total variation," *Journal of Visual Communication and Image Representation*, vol. 30, pp. 181–190, 2015.
- [9] X. Zhang, R. Xiong, X. Fan, S. Ma, and W. Gao, "Compression artifact reduction by overlapped-block transform coefficient estimation with block similarity," *IEEE Transactions on Image Processing*, vol. 22, no. 12, pp. 4613–4626, Dec 2013.
- [10] X. Zhang, R. Xiong, W. Lin, S. Ma, J. Liu, and W. Gao, "Video compression artifact reduction via spatio-temporal multi-hypothesis prediction," *IEEE Transactions on Image Processing*, accepted, to appear, 2015.
- [11] J. Zhang, D. Zhao, R. Xiong, S. Ma, and W. Gao, "Image restoration using joint statistical modeling in a space-transform domain," *IEEE Transactions on Circuits and Systems for Video Technology*, vol. 24, no. 6, pp. 915–928, June 2014.
- [12] H. Liu, R. Xiong, D. Zhao, S. Ma, and W. Gao, "Multiple hypotheses bayesian frame rate up-conversion by adaptive fusion of motion-compensated interpolations," *IEEE Transactions on Circuits and Systems for Video Technology*, vol. 22, no. 8, pp. 1188–1198, Aug 2012.
- [13] X. Zhang, R. Xiong, S. Ma, L. Zhang, and W. Gao, "Robust video super-resolution with registration efficiency adaptation," *Proc. SPIE 7744, Visual Communications and Image Processing*, pp. 774 432(1–8), 2010.